

Droplet Generation by means of a Two-Fluid Probe

Brian P. Cahill^{1,*}, Mandy Quade¹, Gunter Gastrock¹, Karen Lemke¹, Josef Metzger¹ and Dieter Beckmann¹

¹Institut für Bioprocess- und Analysenmesstechnik e.V., Rosenhof, 37308 Heilbad Heiligenstadt, Germany

*Corresponding author: Brian.Cahill@iba-heiligenstadt.de

Abstract: This paper presents a simulation of the operation new type of droplet generation probe. This probe, consisting of two concentrically-arranged tubings, is immersed in a beaker of cell medium so that oil is pumped through the outer tubing at a pumping speed less than fluid is drawn into the inner tubing. In this way, droplets of cell medium are entrained into the outlet tubing forming a segmented flow of homogeneously mixed droplets. The simulation allows the sizing and spacing of the droplets to be ascertained.

Keywords: droplet generation, lab-on-a-chip, digital microfluidics.

1. Introduction

Digital microfluidics is a technique based on the generation, handling, and measurement of droplets. Droplet generation is a necessary step for most high-throughput digital microfluidics applications. The standard droplet generation hardware generates droplets by injecting an aqueous solution into the immiscible oil at a T-junction in a microfabricated chip. The formation of droplets at a T-junction has emerged as a widespread microfluidic tool in the last ten years [1-8] and in particular the application of the technology to cell cultivation [4-8].

A COMSOL simulation of a two-fluid probe for droplet generation is the focus of the work presented here. The T-junction type droplet generation device has been the subject of various simulations [9-10] and serves as an example in the model library of the COMSOL Chemical Engineering module. In Figure 1, the operating principle of the probe is demonstrated: a Teflon tube is placed inside a larger tube and, in Figure 2, a working model of the system is shown. A syringe pump draws fluid into the Teflon tubing at a flow rate greater than oil is pumped into the outer tubing. Thus some cell medium is drawn into the Teflon tubing in the form of droplets.

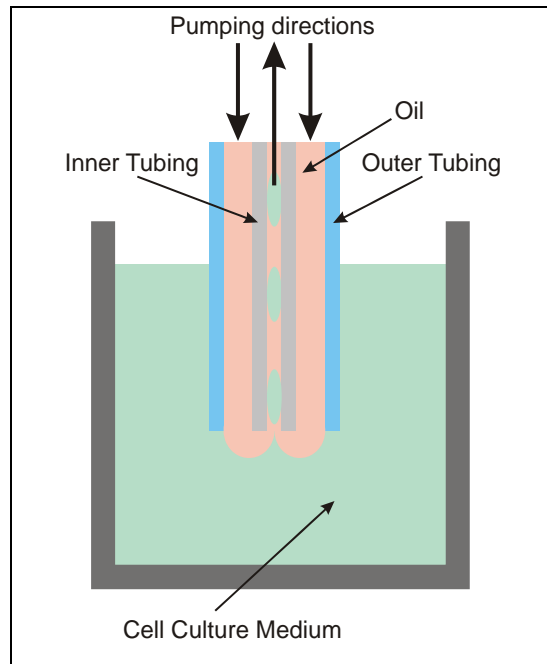


Figure 1. A schematic diagram of the two-fluid probe

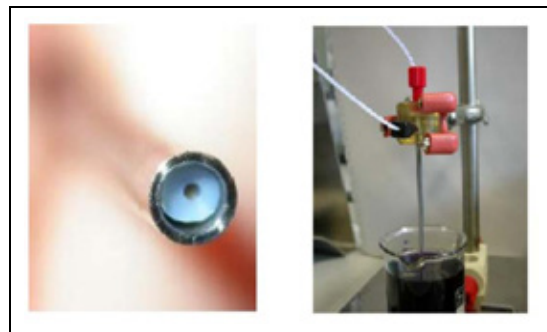


Figure 2. Bottom view and side view of the two-fluid probe

Lemke et al. [11] patented a two-fluid probe that offers significant advantages over the T-junction type droplet generation device which was built into a microdevice for the rapid detection of food pathogens by Schemberg et al. [12]. Firstly, the probe is immersed in cell

culture medium in a beaker, so that the medium can be mixed quite homogeneously by a simple magnetic stirrer. The concentration of the cells or microorganisms in the droplet can be fine tuned to give a high probability of having one cell or microorganism per droplet that is necessary for many biomedical applications. In a microfabricated droplet generator, such as a T-junction, cells are more likely to aggregate together or be trapped at surface inhomogeneities, e.g., at connectors, before they arrive at the T-junction. Secondly, it is relatively simple to fabricate this type of two-fluid probe and, in comparison with microfabricated droplet generators, no expensive clean rooms are required.

2. Use of COMSOL Multiphysics

The geometry of the problem can be simplified quite easily by making use of two-dimensional axial symmetry. The flow in the system is at all times laminar and we chose to implement phase field version of the two-phase flow application mode of the Chemical Engineering module of COMSOL Multiphysics.

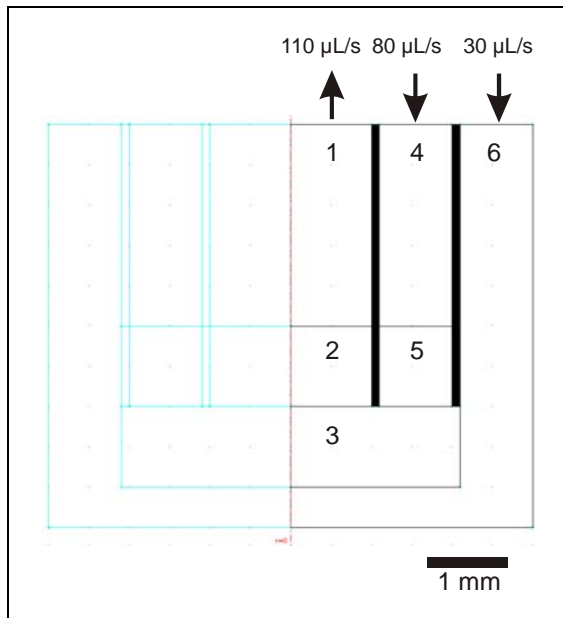


Figure 3. Geometry of the simulation model two-fluid probe

We chose to use the geometry shown above in Figure 3 with water initially filling

subdomains 1, 2, 3 and 6 and tetradecane filling subdomains 4 and 5. The fluid properties of water and tetradecane are given in Table 1.

The boundaries of the tubings are defined as wetted walls. As the inner tubing is in practice always Teflon tubing, we assigned a contact angle of 120° . In two separate simulations we assigned a contact angle of 60° and 120° as the contact angle of the walls of the outer tubing. The walls of the beaker are defined by the no-slip boundary condition. The initial fluid boundary is between the subdomains 3 and 5. The red dashed line above defines the axis of symmetry. The arrows in figure 3 show the laminar outlet and inlet flow rates. The inlet and outlet flow rates are chosen so that their sum is zero.

Table 1: Properties of the fluids used in the simulation.

Water	
Density	1000 kg/m^3
Viscosity	$1.0 \times 10^{-3} \text{ kg/(ms)}$
Tetradecane	
Density	773 kg/m^3
Viscosity	$3.2 \times 10^{-3} \text{ kg/(ms)}$
Surface Tension	$44.2 \times 10^{-3} \text{ N/m}$

3. Results

In Figure 4, the formation of a droplet and its transport through the inner tubing is illustrated. This allows the calculation of droplet size by the performing a volume integral on subdomain 1 with regard to the volume fraction of the aqueous phase. This can be performed from the user interface of COMSOL by choosing “Subdomain Integration” from the Postprocessing menu, choosing “Volume fraction of fluid 1” as the “Predefined Quantity”, clicking the “Compute volume integral (for axisymmetric modes)” box and clicking on “Plot” to solve the integral for each time increment in the simulation.

The volume of aqueous medium in the inner tubing (subdomains 1 and 2 from Figure 2) in the first second of droplet generation is shown for two cases in Figure 5. The first case is for an outer tubing with a contact angle of 60° (hydrophilic) and the second case with a contact

angle of 120° (hydrophobic). The results show how the surface energy of the materials used can affect the size and frequency of droplet generation. In Figure 4 it can be seen how the more hydrophilic outer tubing draws a small amount of aqueous media into the outer tubing so that the phase boundary is drawn a little closer to the inner tubing. In this way droplet breakup happens slightly more quickly so that as the blue curve in Figure 5 shows the droplets are smaller and are generated at a higher frequency than if the outer tubing is made of a more hydrophobic material.

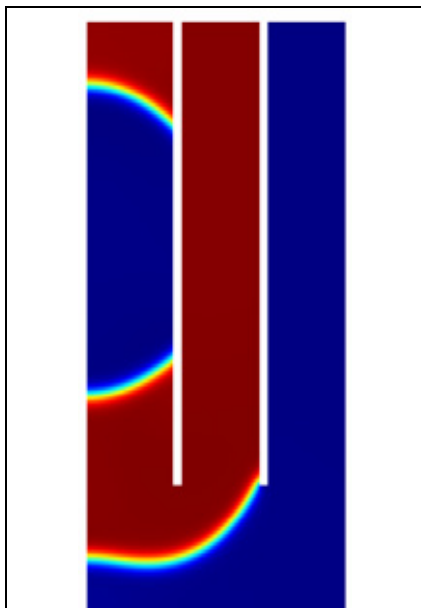


Figure 4. A frame of the simulation showing the passage of a water droplet through the inner tubing

A further geometry was modeled in order to assess the effect of changing the ratio of the flow rate in the inlet tubing to that of the outlet tubing. Figure 6 shows a frame of a simulation of this geometry. The tubings were chosen to have the same inner and outer diameters as that of commonly available tubings, that is, 6 mm / 5 mm and 3.2 mm / 1.6 mm. Figure 6 shows how the droplet is formed by being drawn into the inner tubing and the oil water interface being cut by the surface of the tubing. Once this cut-off takes place the aqueous droplet wets the tubing surface and is drawn into the tubing. Eventually, the oil that is pumped out of the outer tubing accumulates and is drawn into the inner tubing encapsulating the droplet.

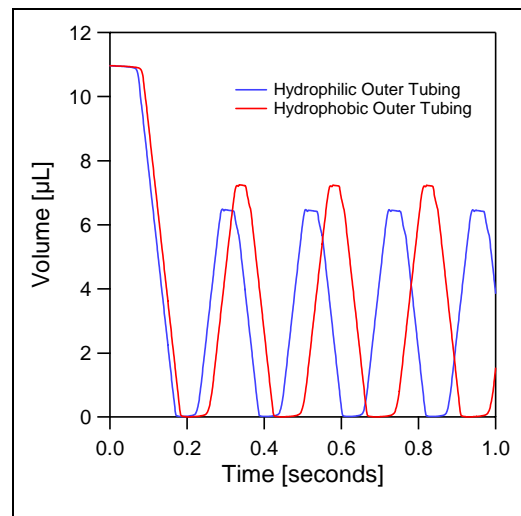


Figure 5. Comparison of the volume of aqueous phase in the inner tubing as a function of time for the cases where the outer tubing is hydrophobic (red curve) and hydrophilic (blue curve).

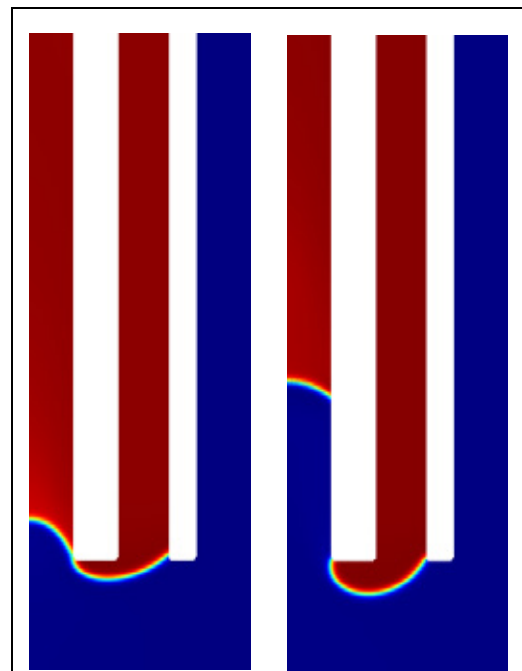


Figure 6. Frames of the simulation showing the formation of a drop at the end of the two-fluid probe and its transit through the inner tubing.

Figure 7 shows the volume of the aqueous phase in the inner tubing as a function of time for various ratios of the flow rate in the inlet tubing to that of the outlet tubing. At all times the flow

rate out of the inner tubing was 200 $\mu\text{L/s}$. In practice, the ratio is often determined by the ratio of the diameters of two syringes being actuated by the same syringe pump.

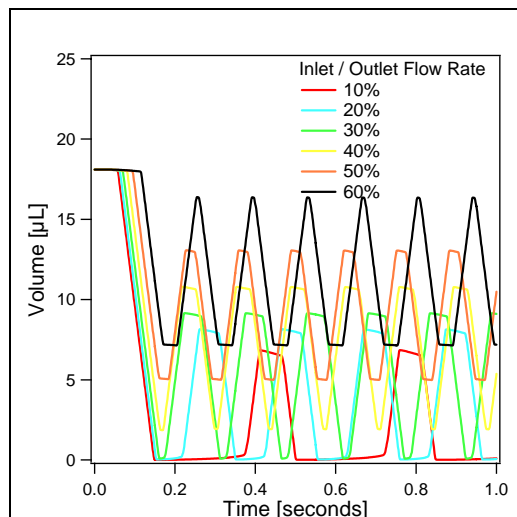


Figure 7. Comparison of the volume of aqueous phase in the inner tubing as a function of time for various ratios of the flow rate in the inlet tubing to that of the outlet tubing for an outlet flow rate of 200 $\mu\text{L/s}$.

Figure 8 shows how the droplet volume decreases as the ratios of the flow rate in the inlet tubing to that of the outlet tubing increases. And how the droplet generation rate reaches a maximum when the flow rate in the input tubing is half that of the flow rate in the output tubing.

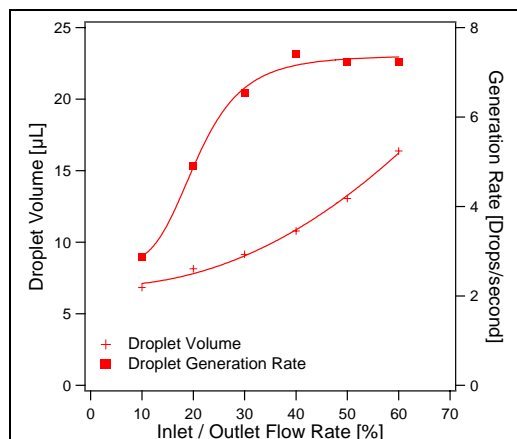


Figure 8. Droplet volume and droplet generation rate as a function of the ratios of the flow rate in the inlet tubing to that of the outlet tubing.

4. Conclusions

Droplet generation is a fundamental tool for digital microfluidics. In order for digital microfluidics to achieve maturity it is necessary to reliably control the generation of droplets. The two-fluid probe offers a way to generate droplets with an optimally mixed cell concentration directly from a beaker. This simulation offers a way to ascertain the size and spacing of droplets in tubing under various flow conditions in a two-fluid probe and for different surface wetting properties of the probe walls.

5. References

1. J. R. Burns and C. Ramshaw, The intensification of rapid reactions in multiphase systems using slug flow in capillaries, *Lab on a Chip*, **1**, 10-15 (2001)
2. T. Thorsen, R. W. Roberts, F. H. Arnold and S. R. Quake, Dynamic Pattern Formation in a Vesicle-Generating Microfluidic Device, *Physical Review Letters*, **86**, 4163-4166 (2001)
3. T. Nisisako, T. Torii and T. Higuchi, Droplet formation in a microchannel network, *Lab on a Chip*, **2**, 24-26 (2002)
4. A. Grodrian, J. Metze, T. Henkel, M. Roth and J. M. Köhler, Segmented flow generation by chip reactors for highly parallelized cell cultivation, *Proc. SPIE*, **4937**, 174-181 (2002)
5. K. Martin, T. Henkel, V. Baier, A. Grodrian, T. Schön, M. Roth, J. Köhler and J. Metze, Generation of larger numbers of separated microbial populations by cultivation in segmented-flow microdevices, *Lab on a Chip*, **3**, 202-207 (2003)
6. A. Grodrian, J. Metze, T. Henkel, K. Martin, M. Roth and J. M. Köhler, Segmented flow generation by chip reactors for highly parallelized cell cultivation, *Biosensors and Bioelectronics*, **19**, 1421-1428 (2004)
7. J. Köhler, T. Henkel, A. Grodrian, T. Kirner, M. Roth, K. Martin and J. Metze, Digital reaction technology by micro segmented flow—components, concepts and applications, *Chemical Engineering Journal*, **101**, 201-216 (2004)
8. T. Henkel, T. Bermig, M. Kielpinski, A. Grodrian, J. Metze and J. Köhler, Chip modules for generation and manipulation of fluid segments for micro serial flow processes,

Chemical Engineering Journal, **101**, 439-445 (2004)

9. J. Liow, Numerical simulation of drop formation in a T-shaped microchannel, *15th Australasian Fluid Mechanics Conference*, (2004)

10. S. van der Graaf, T. Nisisako, C. G. P. H. Schroen, R. G. M. van der Sman and R. M. Boom, Lattice Boltzmann Simulations of Droplet Formation in a T-Shaped Microchannel, *Langmuir*, **22**, 4144-4152 (2006)

11. K. Lemke, G. Gastrock, A. Grodrian, R. Römer, M. Quade, M., D. Roscher, Anordnung und Verfahren zum Erzeugen, Manipulieren und Analysieren von Kompartimenten. *Patent DE 10 2008 039 117.4* (2008)

12. J. Schemberg, A. Grodrian, R. Römer, G. Gastrock and K. Lemke, Online optical detection of food contaminants in microdroplets, *Engineering in Life Sciences*, in press (2009)
doi:10.1002/elsc.200800127

6. Acknowledgements

The authors would like to thank the European Community for financially supporting the FP6 Marie Curie ToK project 29857 InFluEMP.